Antarctic Science 11 (3): 323–331 (1999) © British Antarctic Survey Printed in the United Kingdom

Active tectonics and morphostructure at the northern margin of central Bransfield Basin, Hurd Peninsula, Livingston Island (South Shetland Islands)

J.M. GONZÁLEZ-CASADO[1]*, J. LÓPEZ-MARTÍNEZ[1] and J.J. DURÁN[2]

[1]*Departamento de Química Agrícola, Geología y Geoquímica, Facultad de Ciencias, Universidad Autónoma de Madrid, 28049 Madrid, Spain*

[2]*Instituto Tecnológico Geominero de España, Ríos Rosas 23, 28003 Madrid, Spain*

**G.Casado@uam.es*

Abstract: Geophysical, structural, geomorphological, topographical and bathymetric data from the Hurd Peninsula area, Livingston Island, South Shetland archipelago, suggest that an extensional fault system, orientated NW–SE, together with a conjugate group of NE–SW normal oblique-slip faults, control the landforms in this area. These structures separate fault-bounded blocks of different heights, giving rise to a horst-graben structure. The depressed blocks were filled by glaciers and flooded in part by the sea. The recent movement of these faults can be established from the calculated isopachs of a small Quaternary sedimentary basin, related to this extensional fault system, which shows that sedimentary bed thickness is controlled mainly by the NE–SW fault system. Geomorphological analysis also shows that the NW–SE faults control the main morphostructures of this region. The character of the recent stress tensor has been established from fault-slip data, taking into account only those faults that are related to morphostructures. The calculated palaeostress tensor is extensional, with a N46°E main extension direction, and an average stress ratio of 0.17.

Received 16 July 1998, accepted 28 April 1999

Key words: active tectonics, fracture analysis, geomorphology, geophysical prospecting, palaeostress analysis

Introduction

The South Shetland archipelago is an island arc located approximately 100 km north-west of the Antarctic Peninsula between longitudes 63°W and 54°W, and latitudes 61°S and 63°S, which extends NE–SW more than 500 km from Smith Island to Clarence Island. To the north-west of the archipelago, toward Drake Passage, a wide continental platform gives way to the 4000 m deep South Shetlands Trench (Ashcroft 1972). To the south-east lies Bransfield Basin, a narrow submarine basin (400 x 80 km) up to 2000 m in depth. Beyond Bransfield Strait is the Antarctic Peninsula. Thus, the South Shetland Islands lie between an inactive subduction zone (Maldonado *et al.* 1994) and an incipient back-arc basin (Fig. 1).

At present, small ice caps, each one restrained to a single island, are found in the South Shetland archipelago. Generally, only small peninsulas, capes and points near the seashore are free of ice. The origin and evolution of the landscape in this area is noteworthy because it is probably related to both the tectonic processes and to rapid uplift driven by isostatic compensation related to Quaternary glacial fluctuations.

The aim of this study is to identify the relationship between the geomorphological features of the region, the fracture pattern and the recent stress field. The relationship between fractures and landforms is analysed from local to regional scales. The existence of active tectonics is also addressed by structural, geomorphological and geophysical analysis. We have focused on a region of the northern Bransfield margin on Hurd Peninsula, Livingston Island (Fig. 1b), where there are ice-free areas with topographic, bathymetric and geological data relevant to the present research.

Methods

Because of the extensive ice cover, rock-outcrops are small and discontinuous, which complicates the identification and measurement of large faults in the area. The large amount of snow also makes it difficult to establish the fracture patterns from vertical aerial photographs. Because of this, and in order to determine the regional fracture pattern, potential neotectonic slip directions and the present stress field, the orientation of more than 500 micro- and meso-scale faults (centimetre to metre scale) were measured at 17 sites distributed along the northern part of Hurd Peninsula (Fig. 2). These data are considered statistically representative of the deformation episodes that have taken place in this area.

To deduce which of the fault families could be related to the landforms and thus be recently active we analysed the geomorphological features of the area in order to find lineal morphostructures. These structures were located by a detailed study of the topography (slope analysis), bathymetry and geomorphology.

Faults with the same orientation as the regional linear

https://doi.org/10.1017/S0954102099000413 Published online by Cambridge University Press

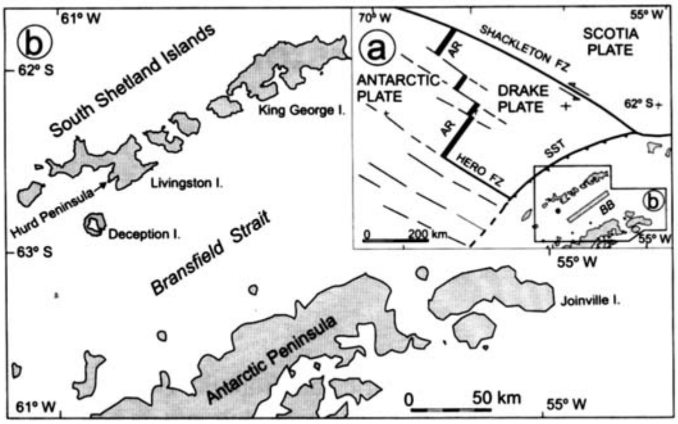

Fig. 1. Location maps. **a.** Sketch map of the South Shetland Islands region. AR: Aluk Ridge (now inactive). BB: Bransfield Basin. SST: South Shetlands Trench. FZ: Fracture Zone (transform faults). **b.** Location of Hurd Peninsula.

morphostructures could be active faults. To verify their neotectonic character, we examined whether or not these faults affect recent materials. Because the most recent rocks in Hurd Peninsula are unconsolidated Quaternary sediments, seismic refraction profiles were made in order to evaluate the possible existence of faults that cut these sediments at depth. The geometry of the metamorphic basement under these sediments has also been studied by means of electrical soundings. The chosen site to investigate the subsurface geometry and the internal structure of the Quaternary sediments was Caleta Española (Spanish Cove, Figs 2 & 3), where there is a relativity large outcrop of Quaternary sediments close to several probably active faults and where the structural features of their surrounding rocks are well known.

This analysis allowed us to choose which fault trends from the measured set are probably active under the present and the recent stress field. Then, by studying these selected faults by means of fault population analysis methods (Pression/Tension diagram, Angelier & Mechler 1977, and Stress Inversion method, Reches 1987) we deduced the orientation and characteristics of the present stress field.

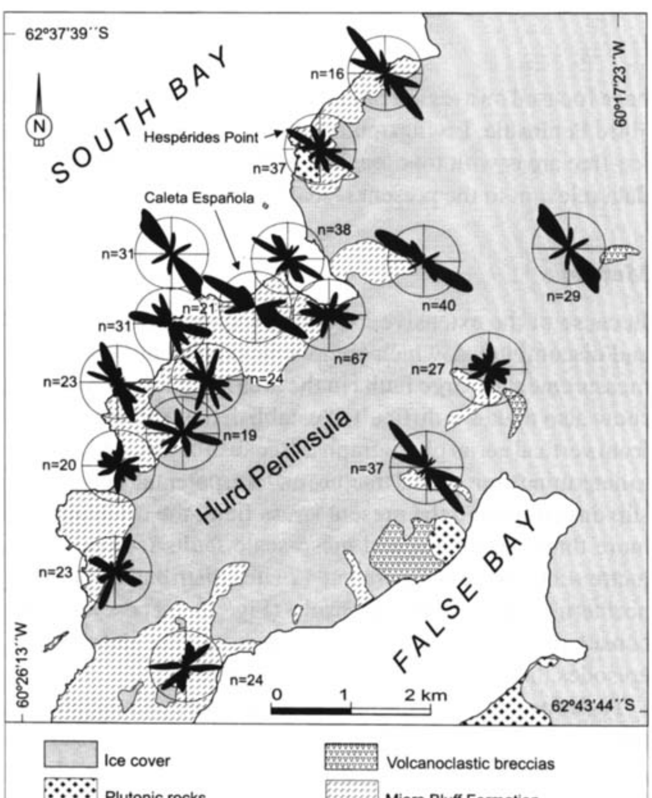

Fig. 2. Geological sketch-map of Hurd Peninsula. The rose diagrams show compilations of fault-plane trends. The circles represent frequencies of 20%. n = number of measured faults.

Geological setting

The islands of the central part of the South Shetland archipelago are mainly composed of calc-alkaline volcanic and plutonic rocks of Cretaceous to Tertiary age. These rocks are part of the magmatic arc generated by subduction processes that took place beneath this margin during the Mesozoic and Cenozoic. Older sedimentary rocks, the Miers Bluff Formation (Permian? to Triassic) on Hurd Peninsula (Fig. 2) and the Byers Group (late Jurassic to early Cretaceous) on Byers Peninsula also crop out on Livingston Island.

The Miers Bluff Formation (e.g. Hobbs 1968, Dalziel 1969, Smellie *et al.* 1984) consists of over 3000 m of alternating greywackes, shales, arkosic arenites, siltstones and minor conglomerates (Arche *et al.* 1992, Pallàs *et al.* 1992). Many of the lithologies exhibit features characteristic of turbidites. A Permo–Triassic age has tentatively been assigned to this formation by correlation with similar sequences of the Antarctic Peninsula (Trinity Peninsula Group) and by stratigraphical dating of some fossil plant remains. On the north-west margin of False Bay (Fig. 2), a heterogeneous group of rocks outcrops composed mainly of volcanoclastic breccias. These beds are stratigraphically above the Miers Bluff Formation and a probable Cretaceous age has been assigned to them (Smellie *et al.* 1995). Some small stocks of granitic rocks are also visible at Hespérides Point and False Bay (Fig. 2). The tonalitic rocks of Hespérides Point have been dated as late Cretaceous (73 ± 3 Ma, K–Ar whole rock, Kamenov 1997). In the study area, all the previously described lithologies are intruded by basic dykes of probable Jurassic–Cretaceous age (Willan 1994, Willan *et al.* 1994). In many places these rocks are covered by Quaternary deposit including matrix-poor moraines formed of boulders and cobbles, slope debris, raised marine beaches consisting of well-rounded pebbles with sand and silty matrix and small alluvial and talus cones (Fig. 3).

Near Caleta Española (Figs 2 & 3), the Miers Bluff Formation crops out as metre to decametre scale beds with a dominant NE–SW strike and an average dip of 40° to the NW. The main

https://doi.org/10.1017/S0954102099000413 Published online by Cambridge University Press

structures on Hurd Peninsula are folds with sub-horizontal axial planes, and, thus, in many places the beds are overturned (Dalziel 1972), e.g. in the area around the Spanish Antarctic station (Fig. 3). The previous structural and geological accounts of Hurd Peninsula (e.g. Willan 1994, Pallàs 1996) as well as our detailed study of Caleta Española (Fig. 3) show that the folded beds are crosscut by two sets of faults. One set is orientated NW–SE, with an oblique normal sense of slip, and some show recent activity (Pallàs *et al.* 1995, González-Casado *et al.* 1997, Bergamín *et al.* 1997). The other set are orientated NE–SW and usually shows an oblique sense of movement. Small tectonic blocks of different heights probably result from the conjugate displacement along both groups of faults (Bergamín *et al.* 1997).

Plate tectonic setting

In this region two main geotectonic processes are taking place (Fig. 1a):

1) Bransfield Basin is probably in the first stages of opening as an oceanic basin. Seismic profiles and the bathymetry show clear evidence of extensional structures (e.g. Gràcia *et al.* 1996, 1997, Lawver *et al.* 1996, Canals *et al.* 1997, Prieto *et al.* 1997). Seismic reflection profiles show the presence of a thick sedimentary cover over an acoustic basement. The basement is strongly normal-faulted giving a half-graben structure. The seismic data allow calculation of the extension of the crust by more than 25% (González-Casado *et al.* 1997). Bransfield Basin contains the Quaternary subaerial volcanic edifices of Deception, Bridgeman and Penguin islands. Also, the seismic profiles show several submarine volcanic edifices, some of them probably active (Gràcia *et al.* 1996, 1997, Lawver *et al.* 1996, Canals *et al.* 1997). The geochemical character of these volcanoes is not uniform; some (e.g. Deception Island) resemble subduction generated magmas (e.g. Aparicio *et al.* 1997) while dredge samples from several points within the basin are similar to Pacific back-arc basins (Lawver *et al.* 1996). There are, probably, two different magmatic reservoirs. The existence of incipient oceanic crust in the Bransfield Basin is subject to debate since the thickness of the crust suggests that normal seafloor spreading has yet to occur. The tectonic model for this basin is not well-determined.

2) The South Shetlands Trench was a subduction zone that permitted convergence between the oceanic Phoenix Plate and the Antarctic Plate during the Mesozoic and Cenozoic. Convergence seems to have finished 4 m.y. ago when the expansion centre of the Phoenix Plate (the Aluk Ridge) became inactive. The remnant of the former Phoenix Plate has been named the Drake Plate by some authors (e.g. Herron & Tucholke 1976). At present, the moderate tectonic and seismic activity that is observed in this zone seems to be related to trench rollback (Barker 1982, Barker & Dalziel 1983, Maldonado *et al.* 1994, Lawver *et al.* 1995, 1996). During active subduction numerous aseismic ridges and transform faults with a NW–SE trend were formed (Fig. 1a).

Recent and present stress tensors in this region

From studies of earthquake focal mechanisms (Pelayo & Wiens 1989, fig. 6, focal mechanism of events 5 and 14) and fault population analysis from Deception Island (González-Casado *et al.* 1997), it seems well-established that in the Bransfield Basin domain (Fig. 1) the present stress tensor is extensional, with σ_1 subvertical and σ_3 subhorizontal with a NW–SE trend (extension direction). This orientation of extension is perpendicular to the axis of the Bransfield Basin and congruent with NE–SW trending normal faults that are observed in the ocean floor and in Deception Island.

In the South Shetlands tectonic block there are no determinations of earthquake focal mechanisms, but previous studies of fracture analyses on Hurd Peninsula (e.g. Sàbat *et al.* 1992, Santanach *et al.* 1992, 1996, Willan 1994) have established an extensional stress tensor, with a subhorizontal extension direction orientated NW–SE. These authors also agree that prior to this extensional episode two fracturing events with strike-slip stress tensors occurred (i.e. σ_1 and σ_3 subhorizontal). In the oldest phase, σ_1 was orientated NW–SE and σ_3 NE–SW, while in the intermediate episode the orientations of the axes were transposed, with σ_1 orientated NE–SW and σ_3 NW–SE. These older fracturing episodes

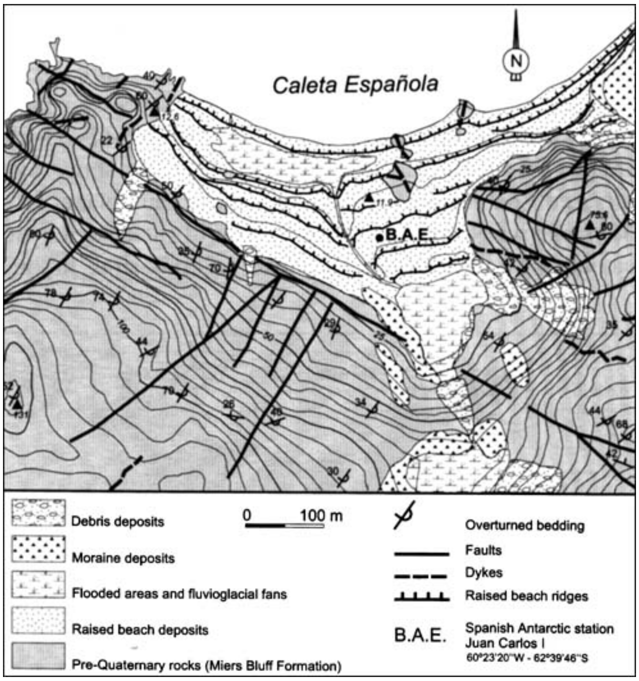

Fig. 3. Geological map of the Caleta Española area. Height in metres; contour interval = 5 m.

https://doi.org/10.1017/S0954102099000413 Published online by Cambridge University Press

were related to a strike-slip regime probably associated with the convergent movement between the Phoenix and the Antarctic plates. In the previously cited works the criteria for establishing the relative chronology between the deduced stress tensors was mainly cross-cutting fault relationships. The number of faults used in the stress tensor determinations was, however, very low.

In the South Shetlands Trench there is a single focal mechanism determination, which shows normal faulting and the same stress axes orientation as those of the Bransfield domain (Pelayo & Wiens 1989, fig. 6, event 15).

Neotectonic analysis

The neotectonic analysis in this study is based upon a three-step method. We first determined the regional fracture pattern, then selected the possible active faults by comparing fault trends with the orientations of recent morphostructures, and, finally, established whether or not these faults cut through Quaternary deposits.

Fracture pattern

The 507 measured faults, distributed over 17 sites on the Hurd Peninsula (Fig. 2), have a principal NW–SE (N 125°E) trend (Figs 2 & 4), although NNE–SSW and NNW–SSE trends are also present. The faults are characterized by their steep dip with more than the 75% of the faults having a dip greater than 60° (González-Casado *et al.* 1997). For all the faults the direction of slip was established using asymmetric features observable on the fault surface, e.g. mineral steps, alternating polished and rough facets and conjugate shear fractures. A subdivision of faults based on slip shows that oblique slip faults are the most abundant (normal oblique-slip = 55%, reverse oblique-slip = 22%) followed by strike-slip faults (12%). Normal dip-slip (9%) and reverse dip-slip (1%) faults are less abundant. Thrusts are absent. All faults show small offsets of some tens of centimetres. Some fault planes have been reactivated and they show two sets of slickensides with incompatible sense of slip, e.g., dextral and sinistral. In some cases it is difficult to deduce the slip order from the cross-cutting relationship because different faults have a distinct relative order. The rocks cut by these structures are mainly Permian? to Triassic metasediments of the Miers Bluff Formation. However, faults that cut the dykes and the granitic rocks were also measured.

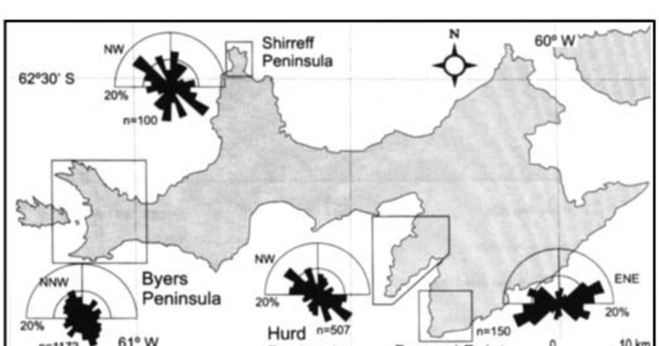

Fig. 4. Fracture patterns in several places of Livingston Island. n = number of measured faults or lineaments.

A complementary study of fracturing has also been made in other places of Livingston Island: Shirreff Peninsula and Barnard Point (González-Casado *et al.* 1997). As shown in Fig. 4, Shirreff Peninsula is also dominated by a NW–SE fracture direction. However, towards Bransfield Strait the ENE–WSW orientation becomes more dominant. The orientation of more than 1000 photo-interpreted linear structures measured on Byers Peninsula by López-Martínez *et al.* (1996) also show NNW–SSE and NW–SE main trends. Taking into account the statistical distribution (rose diagrams of Fig. 4) of the faults in Livingston Island, two dominant groups of orientation can be seen: NW–SE and NE–SW, which are sub-parallel to the main geotectonic elements of this region, that is, transform faults, ridges and trenches.

Morphostructural analysis

To establish the location of the morphotectonic elements in the area (neotectonic faults) an extensive analysis of topography (Servicio Geográfico del Ejército 1991) was carried out near the Spanish station Juan Carlos I (B.A.E.). The slope-map (Fig. 5) shows clearly that the steep slopes are orientated NE–SW and NW–SE and delimit small blocks with relatively flat tops. The steep slopes correspond to coastal cliffs, slopes of glacial valleys and abrupt mountain crests. Although every one of these landforms has a different origin, we consider that all of them relate to recent tectonic movement because they are straight and continuous, they separate areas with different relief and, they are sub-parallel to the observed main fault trends.

The sea-floor morphology of this region also displays abundant morphostructures with NW–SE and NE–SW orientations. A recent bathymetric map of the seafloor around Hurd Peninsula (Servicio Geográfico del Ejército 1997) shows several scarps on the seafloor, with steep slopes more than 75 m high (Fig. 6). The scarps trend NW–SE and in some cases are up to 15 km in length. Some of the submerged features have been interpreted as moraine ridges and terminal moraines that are related to glacio-eustatic sea level rise (e.g. Pallàs *et al.* 1995). The submarine troughs also have the same NE–SW and NW–SE trends. These facts, may indicate the genetic relationship between the orientation of the faults and the geomorphological features. In small bays close to the coast (e.g. Johnson Dock, Fig. 5) the bathymetry shows submerged arch-like forms made of sediments. These arches are probably related to older steps in the basement rocks (possibly fault scarps) generated during the displacement of NE–SW and NW–SE faults.

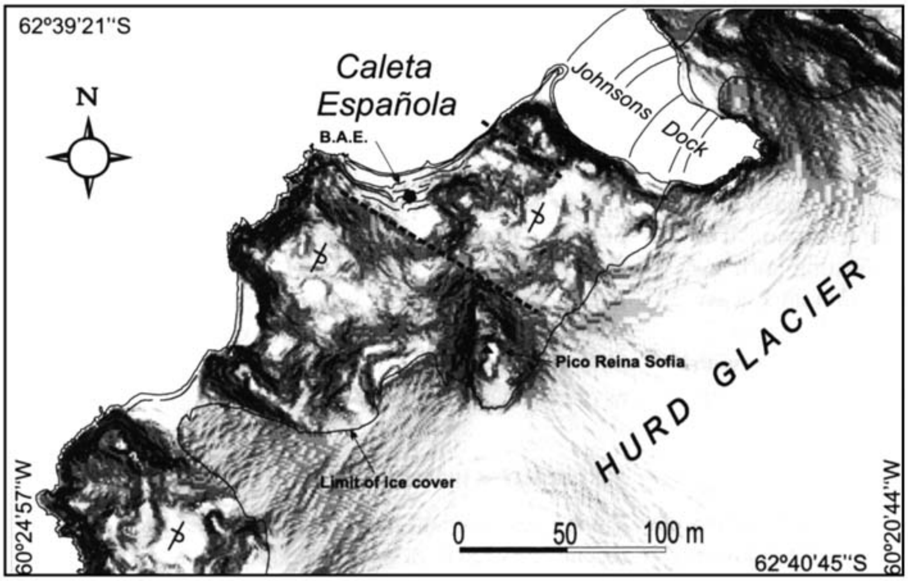

Fig. 5. Slope map of north-western Hurd Peninsula. The intensity of grey in each point indicates the slope (from 0° to 77°, centesimal degrees). B.A.E.: Spanish Antarctic station Juan Carlos I. Some NW–SE lineations that delimit flat top blocks have been highlighted. Also shown are the ice margin, some submarine arches in Johnsons Dock, and raised beaches. Digitalized topography from the topographic map of the area at 1:5000 scale (Servicio Geográfico del Ejército 1991).

Geophysical prospecting in the Caleta Española area

To determine whether the faults in the area were recently active, we require evidence that they cut recent materials. However, the lack of consolidated Quaternary sedimentary rocks makes it very difficult to find such faults. Furthermore, any possible surface fault-scarps that developed in these materials would tend to be destroyed rapidly by erosion in the present glacial and periglacial environment. One way to investigate the presence of faults that cut Quaternary sediments is through a geophysical study. We therefore studied the geometry of the basement rocks below a small basin of Quaternary deposits along with the internal structure of the deposits themselves.

The results of the resistivity study of the Caleta Española Quaternary basin (Bergamín *et al.* 1997) show that the sediments and the basement rocks have very different resistivities. This allows us to establish the basement geometry below the sediments. The calculated shape for the basin is a narrow, deep trough with a NW–SE orientation, i.e. parallel to the main faults of the region (Fig. 7). The trough reaches a depth of 70 m below sea level and it has a small asymmetric threshold in the vicinity of its coastal side. This is consistent with the two sets of observed fractures orientated NW–SE and NE–SW (Fig. 3). Given the depth and steep sides of the basin, a tectonic origin seems very probable. Nevertheless, after its tectonic initiation, the trough could have been deepened even

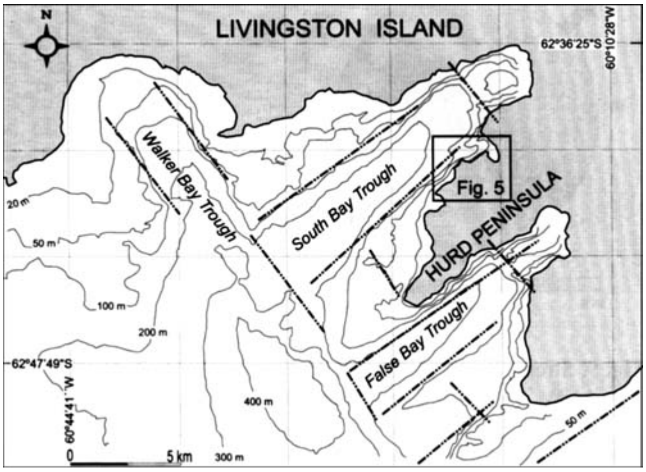

Fig. 6. Bathymetric map in the vicinity of Hurd Peninsula from Servicio Geográfico del Ejército (1997). Dotted lines represent main seafloor steps. Inset box shows area of Fig. 5.

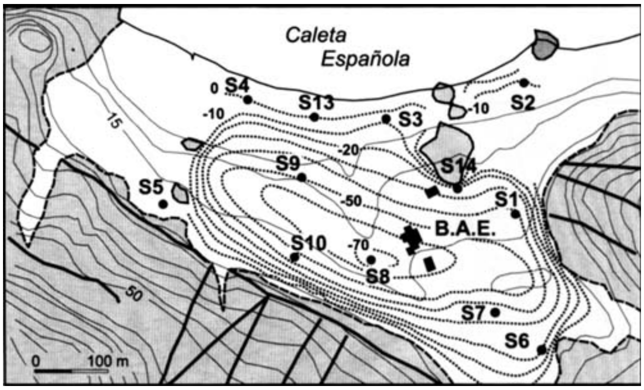

Fig. 7. Contours on top of basement (isobath) below the Quaternary deposits in the Caleta Española, based on the interpretation of the electric soundings (S1 to S13). Dashed lines are isobaths corresponding to the basement surface below the Quaternary sediments, values in metres below sea level, contour interval = 10 m. Miers Bluff Formation outcrops are shown in grey. Topographic contour interval = 5 m. Thick lines represent faults.
B.A.E. = Spanish Antarctic station Juan Carlos I.

https://doi.org/10.1017/S0954102099000413 Published online by Cambridge University Press

further by glacial erosion. Glacial flow from the ESE was possible as is shown by moraines and glacial abrasion marks.

The internal structure of the Quaternary beds was examined in several sledge-hammer seismic refraction profiles. Most of the lines ran parallel to the bedrock trough (1150 m surveyed) and the others were orientated perpendicular to this structure (550 m surveyed). This more-or-less rectangular grid of lines enabled us to obtain three-dimensional information. The interpretation of the results shows three reflecting horizons that separate two layers characterized by a different P-wave velocity ($V_1 \approx 450$ ms^{-1} and $V_2 \approx 1700$ ms^{-1}) and an acoustic basement ($V_3 \approx 4500$ ms^{-1}). Based on the correlation with observations made in a small trench (*c.* 3 m deep) and with the results of the resistivity soundings, these layers could be identified as beds of sediment. The thickness of the upper layer coincides with that of the first level detected in the vertical electric soundings, and is interpreted as the permafrost and the active soil layer. Comparing the depth of the lower seismic layer with the basement depth deduced from the electrical soundings, we infer that some parts of the seismic profiles did not reach bedrock.

The isopach map of the upper layer (Fig. 8a) shows relatively thicker areas close to the limits of the basin (dashed lines of Fig. 8a), which could correspond to debris cones. Other contours are aligned NE–SW, nearly parallel to the NE–SW fault set. The lower layer shows frequent variations in thickness with maxima and minima that appear as a sequence of narrow bands orientated NE–SW (Fig. 8b), similar to the trends of faults that outcrop to the south (Fig. 3). There are also some bands with a NW–SE orientation.

The similarity in orientation between the NE–SW faults and the calculated isopach trends suggests a relationship between them, particularly in the case of the lower layer. One interpretation of the isopachs is to consider that the NE–SW faults controlled the deposition of these beds. Some of the other trends, however, could have other interpretations such as old drainage systems or debris cones.

Recent stress tensor

Taking into account the previous results, we calculated the recent stress axis orientations using only faults that have trends close to those of the principal morphotectonic directions. Thus, we analysed faults orientated within an interval of 50° around the main directions: N30°E and N130°E, i.e., between N5°E and N55°E, and between N105°E and N155°E.

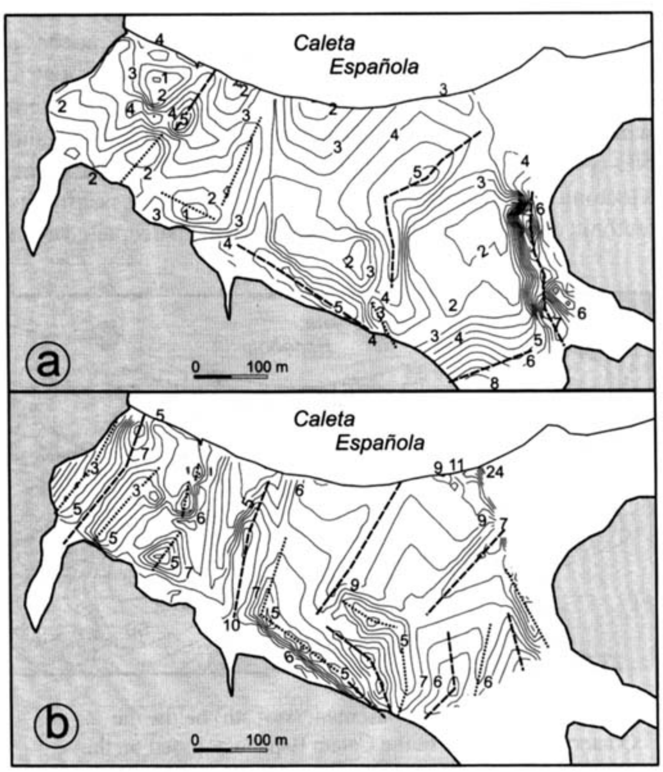

Fig. 8. a. Isopach map of the upper seismic layer ($V_1 \approx 450$ ms^{-1}), contour interval = 0.5 m. **b.** Isopach map of the lower seismic layer ($V_2 \approx 1700$ ms^{-1}), contour interval = 1 m. Dashed lines show trends of maximum thickness; dotted lines show trends of minimum thickness. Miers Bluff Formation outcrops are shown in grey.

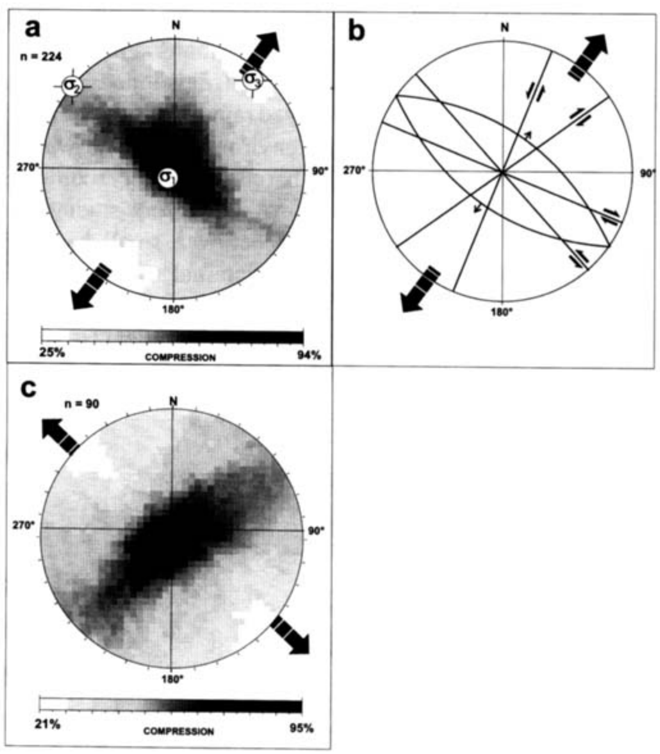

Fig. 9. Stress tensor. **a.** Results of the stress analysis for NE–SW and NW–SE faults. The shading shows the cumulative probability that the p-axis will lie in a particular field. The positions of the principal stresses are deduced from the Reches method. Arrows represent the horizontal extension direction. *n* = number of measured faults. **b.** Main fault orientations and their theoretical movement. **c.** Results of the stress analysis for NE–SW faults.

https://doi.org/10.1017/S0954102099000413 Published online by Cambridge University Press

With this set of faults (224 faults), an average orientation of the principal stresses, σ_1 and σ_3, was calculated using the right dihedra method (Angelier & Mechler 1977). This method relies on the assumption that all the faults slip together under a single, uniform stress tensor. In consequence, calculating the focal mechanism for each fault makes it possible to find areas of compression (P) and tension (T) common to the entire fault set. The principal stresses are located inside these areas. No information about the stress ratio or timing of fault slip episodes can be obtained. The resulting compilation is shown in Fig. 9a. The position of the maximum compression region is represented by the black area of Fig. 9a, and the minimum compression by the white area. The maximum shortening direction is nearly vertical and the minimum shortening direction is almost horizontal and orientated NE–SW. Then, the maximum horizontal stress (S_{HMAX}) is orientated NW–SE.

To find the stress tensor that fits the slip of the selected set of faults and striae with a minimum misfit we used the stress inversion method proposed by Reches (1987). Like other fault population analysis methods (e.g. Angelier 1979, Etchecopar *et al.* 1981), it relies on the Wallace-Bott relationship, which states that the slip along a fault takes place in the direction of the maximum resolved shear stress (Wallace 1951, Bott 1959), but also assumes the Navier-Coulomb rupture principle. This method allows calculation of the orientation and relative magnitudes of σ_1, σ_2 and σ_3, their axial ratio ($R = (\sigma_2 - \sigma_3) / (\sigma_1 - \sigma_3)$), and the misfit angle between the measured and the calculated striae. The selected solution was that which fit the largest number of faults with the minimum error. We calculated a stress tensor with the principal stress axes as follows: $\sigma_1 = 86/210$, $\sigma_2 = 0/316$ and $\sigma_3 = 3/46$ (Fig. 9a), an axial ratio of 0.17 and an average misfit angle of 33°, which fits 56.4 % of the analysed faults. The obtained principal stress axes orientations agree with the orientation of the maximum compression and tension areas deduced from the right dihedra method (Fig. 9a).

Under this stress orientation, the NW–SE trending faults probably moved recently as normal faults, giving rise to the biggest fault scarps, whereas the NE–SW faults moved as oblique normal-slip faults (Fig. 9b).

Discussion and conclusions

As has been previously pointed out (López-Martínez *et al.* 1992a, 1992b, Pallàs *et al.* 1995), the shape of Hurd Peninsula and many of its landforms seems to be tectonically controlled. According to Pallàs *et al.* (1995) Hurd Peninsula is divided into several tectonic blocks without a regular pattern (Pallàs *et al.* 1995, Figs 3 & 4), although they found that one of the main neotectonic fault orientations was NE–SW. They analysed aerial photographs to identify lineations and morphoneotectonic features, and they considered these lineations to be due to recent fault displacement based on geomorphological considerations.

The fracture analysis carried out in this study allows us to conclude that the NW–SE and NE–SW trends are the characteristic fault orientations on the island, being present in several different places. The same orientations are evident in different geomorphological features (steep slopes, moraines, mountain crests, coastal cliffs and glacial troughs), and also in the sea-floor morphology, e.g. deep off-shore troughs and sea-floor steps. Thus, there is a correlation between fracture patterns and morphological elements. These faults appear to have been recently active. Thus, Hurd Peninsula and its surroundings are divided into several tectonic blocks, bounded by faults trending NW–SE and NE–SW, which have a regular pattern (Fig. 10). This model could explain the succession of NE–SW troughs and peninsulas (i.e. South Bay trough, Hurd Peninsula, False Bay trough, Barnard Point) as a succession of horst and graben structures.

The recent stress tensor (Fig. 9a) has been calculated assuming that the two main fault trends (NE–SW and NW–SE) moved under the same deformation episode. However, the possibility that both fault systems were related to two different discrete episodes of deformation needs to be considered. The strong NE–SW trend in the Quaternary sediment isopachs at Caleta Española suggests that the NE–SW faults could have moved more recently. In this sense, the principal stress orientation has been calculated only for this fault family (Fig. 9c), which enables us to infer a NW–SE extension direction. Thus, two discrete episodes of fracturing with different orientations of their extension directions, NE–SW and NW–SE, can be deduced.

It is difficult to choose between these two possibilities, and when our study is compared with previous works, some discrepancies can be found. The calculated extensional stress tensor that fits both fault directions (Fig. 9a) does not agree with the recent stress tensor calculated by Santanach *et al.* (1992, 1996) in this same area. Both tensors are extensional (σ_1 sub-vertical), but the positions of σ_2 and σ_3 are transposed. Santanach *et al.* (1992, 1996) established a NW–SE extension direction that agrees with our second possibility. Nevertheless, these differences could be due to the way in which the faults used in calculating the stress tensor were selected. We selected faults on the basis of geomorphological criteria, while Santanach *et al.* (1992, 1996) worked with an iterative method of fault population analysis (e.g. Etchecopar *et al.* 1981) that allowed them to establish three tensors for a small group of faults measured in one site. Moreover, the calculated NW–SE extension direction also shows a good correlation with the principal stress orientation established for tectonic units located to the south (Bransfield Basin, Pelayo & Wiens 1989, Galindo-Zaldivar *et al.* 1996, González-Casado *et al.* 1997) and to the north (South Shetlands Trench, Pelayo & Wiens 1989). In all these areas one principal stress axis is sub-vertical (σ_1) and the other two (σ_2 and σ_3) are sub-horizontal with NE–SW and NW–SE orientations. Taking into consideration this other data, the two successive episodes of deformation appear to be the most appropriate possibility. Although reversal in the principal stress orientation has been reported in tectonic environments where there are changes in the stress regime in contiguous regions (e.g. Mattauer & Mercier 1980, Sassi & Faure 1996, De Vicente *et al.* 1996). These reversals are a common feature on arc back-arc regions (e.g. Nakamura & Uyeda 1980, Froidevaux *et al.* 1988). In this case, and given the close values between σ_2 and σ_3 ($R = 0.17$), the reversal could be caused by forces transmitted to the South Shetland tectonic block from the adjacent tectonic units.

The NW–SE fracture system is parallel to the transform faults of the Drake and Antarctic plates and are more ubiquitous towards the South Shetlands Trench, i.e. in the central and northern parts of Livingston Island (Fig. 4). The NE–SW faults are subparallel to the Bransfield ridge and fractures are more important in the south part of Livingston Island (Fig. 4). Consequently, in the northern part of Livingston Island, a NE–SW extension is prevalent and in the southern area, the extension is normally orientated NW–SE, while in the middle sector it is possible to find both extension directions (Fig. 10). This agrees with the tectonic setting because the NW–SE extension in southern Livingston Island is compatible with the incipient back-arc spreading in Bransfield Basin, and the NW–SE maximum shortening direction, dominant in the northern part of the island, is compatible with the NW–SE tectonic force transmitted to the South Shetland tectonic block from the adjacent Drake Plate.

Acknowledgements

Financial support for this work was provided by the Spanish Interministerial Commission of Science and Technology (CICYT) research projects ANT94-0666 and ANT98-0225 of the Spanish Antarctic Research Program. This paper is dedicated to the memory of J.F. Bergamín who passed away in August 1997, while this contribution was in preparation. He participated in the field work, obtaining the geophysical data. The paper has benefited greatly from the referee comments by Dr J. Bradshaw and Dr A. Densmore. We also thank Dr M.R.A. Thomson of the British Antarctic Survey for his useful suggestions and comments.

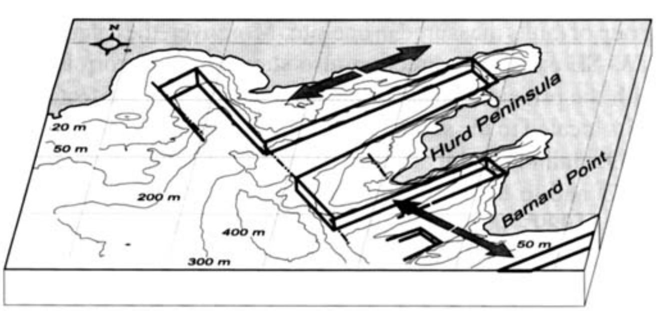

Fig. 10. Proposed fault movement model. Arrows represent the main extension directions.

References

Angelier, J. 1979. Determination of the mean principal stresses for a given fault population. *Tectonophysics*, **56**, T17–T26.

Angelier, J. & Mechler, P. 1977. Sur une méthode graphique de recherche des constraintes principales également utilisable en tectonique et en seísmologie: le méthode des dièdres droits. *Bulletin Société Géologique de France*, **7**, 1309–1318.

Aparicio, A., Risso, C., García, A., Ortiz, R. & Astiz, M. 1997. Esquema geodinámico del volcanismo de la Isla Decepción (Islas Shetland del Sur). *Boletín de la Real Sociedad Española de Historia Natural (Sección Geológica)*, **93**, 155–161.

Arche, A., López-Martínez, J. & Marfil, R. 1992. Petrofacies and provenance of the oldest rocks in Livingston Island, South Shetland Islands. *In* López-Martínez, J., *ed. Geología de la Antártida Occidental*. Simposios T 3. Salamanca: III Congreso Geológico de España y VIII Congreso Latinoamericano de Geología, 141–151.

Ashcroft, W.A. 1972. Crustal structure of the South Shetland Islands and Bransfield Strait. *British Antarctic Survey Scientific Reports*, No 66, 43 pp.

Barker, P.F. 1982. Cenozoic subduction history of the Pacific margin of the Antarctic Peninsula: ridge crest-trench interactions. *Journal of the Geological Society, London*, **139**, 787–801.

Barker, P.F. & Dalziel, I.W.D. 1983. Progress in geodynamics in the Scotia Arc region. *In* Cabre, R., *ed. Geodynamics of the eastern Pacific region, Caribbean and Scotia arcs*. Geodynamics Series, vol. 9. Washington, DC: American Geophysical Union, 137–140.

Bergamín, J.F., Durán, J.J., González-Casado, J.M. & López-Martínez, J. 1997. Morfología y estructura del basamento precuaternario de la Caleta Española, Península Hurd, Isla Livingston. *Boletín de la Real Sociedad Española de Historia Natural (Sección Geológica)*, **93**, 89–196.

Bott, M.H.P. 1959. The mechanics of oblique slip faulting. *Geological Magazine*, **96**, 109–117.

Canals, M., Gràcia, E. & GEBRA Group. 1997. Evidence of initial seafloor spreading in the Central Bransfield Basin, Western Antarctica. *Boletín de la Real Sociedad Española de Historia Natural (Sección Geológica)*, **93**, 53–61.

Dalziel, I.W.D. 1969. Structural studies in the Scotia Arc: Livingston Island. *Antarctic Journal of the United States*, **4**(4), 1–137.

Dalziel, I.W.D. 1972. Large-scale folding in the Scotia arc. *In* Adie, R.J., *ed. Antarctic geology and geophysics*. Oslo: Universitetsforlaget, 47–55.

De Vicente, G., Giner, J., Muñoz-Martín, A., González-Casado, J.M., & Lindo, R. 1996. Determination of present-day stress tensor and neotectonic interval in the Spanish Central System and Madrid Basin, central Spain. *Tectonophysics*, **266**, 405–424.

Etchecopar, A., Vasseur, G. & Daignères, M. 1981. An inverse problem in microtectonics for the detemination of stress tensor from fault striation analysis. *Journal of Structural Geology*, **3**, 51–65.

Froidevaux, C., Uyeda, S. & Uyeshima, M. 1988. Island arc tectonics. *Tectonophysics*, **148**, 1–19.

Galindo-Zaldivar, J., Jabaloy, A., Maldonado, A. & Sanz de Galdeano, C. 1996. Continental fragmentation along the South Scotia Ridge transcurrent plate boundary (NE Antarctic Peninsula). *Tectonophysics*, **259**, 275–301.

González-Casado, J.M., López-Martínez, J., Durán, J.J. & Bergamín, J.F. 1997. Fracturación y campos de esfuerzos recientes en el entorno del Estrecho de Bransfield. *Boletín de la Real Sociedad Española de Historia Natural (Sección Geológica)*, **93**, 181–188.

Gràcia, E., Canals, M., Farràn, M., Prieto, M.J., Sorribas, J. & GEBRA team. 1996. Morphostructure and evolution of the Central and Eastern Bransfield basins (NW Antarctic Peninsula). *Marine Geophysical Researches*, **18**, 429–448.

GRÀCIA, E., CANALS, M., FARRÀN, M., SORRIBAS, J. & PALLÀS R. 1997. Central and Eastern Bransfield Basins (Antarctica) from high-resolution swath-bathymetry data. *Antarctic Science*, **9**, 168–180.

HERRON, E.M. & TUCHOLKE, B.E. 1976. Sea-floor magnetic patterns and basement structure in the southeastern Pacific. *In* HOLLISTER, C.D. *et al., Initial Reports of the Deep-Sea Drilling Project,* **35**. Washington, DC: US Government Printing Office, 263–278.

HOBBS, G.J. 1968. The geology of the South Shetland Islands: IV. The geology of Livingston Island. *British Antarctic Survey Scientific Reports*, No. 47, 34 pp.

KAMENOV, B.C. 1997. Geochemistry and petrology of the Hesperides Point Intrusion, Hurd Peninsula, Livingston Island. *In* RICCI C.A., *ed. The Antarctic region: geological evolution and processes.* Siena: Terra Antartica Publication, 341–352.

LAWVER, L.A., KELLER, R.A., FISK, M.R. & STRELIN, J.A. 1995. Bransfield Basin, Antarctic Peninsula: active extension behind a dead arc. *In* TAYLOR, B., *ed. Back arc basins: tectonic and magmatism.* Amsterdam: Plenum Press, 315–342.

LAWVER, L.A., SLOAN, B.J., BARKER, D.H.N., GHIDELLA, M., VON HERZEN, R.P., KELLER, R.A., KLINKHAMMER, G.P. & CHIN, C.S. 1996. Distributed, Active Extension in Bransfield Basin, Antarctic Peninsula: evidence from multibeam bathymetry. *GSA Today*, **6-11**, 1–6.

LÓPEZ-MARTÍNEZ, J., MARTÍNEZ DE PISÓN, E. & ARCHE, A. 1992a. Geomorphology of Hurd Peninsula, Livingston Island, South Shetland Islands. *In* YOSHIDA, Y., KAMINUMA, K. & SHIRAISHI, K., *eds. Recent progress in Antarctic earth science*. Tokyo: Terrapub, 751–756.

LÓPEZ-MARTÍNEZ, J., VILAPLANA, J. M., MARTÍNEZ DE PISÓN, E., CALVET, J., ARCHE, A., SERRAT, D. & PALLÀS, R. 1992b. Geomorphology of selected areas in Livingston Island, South Shetland Islands. *In* LÓPEZ-MARTÍNEZ, J., *ed. Geología de la Antártida Occidental.* Simposios T-3. Salamanca: III Congreso Geológico de España y VIII Congreso Latinoamericano de Geología, 271–281.

LÓPEZ-MARTÍNEZ, J., HATHWAY, B., LOMAS, S., MARTÍNEZ DE PISÓN, E. & ARCHE, A. 1996. Structural geomorphology and geological setting. *In* LÓPEZ-MARTÍNEZ, J., THOMSON, M.R.A. & THOMSON, J.W., *eds. Geomorphological map of Byers Peninsula, Livingston Island.* BAS GEOMAP Series, Sheet 5-A. Cambridge: British Antarctic Survey, 9–14.

MALDONADO, A., LARTER, R.D. & ALDAYA, F. 1994. Forearc tectonic evolution of the South Shetland Margin, Antarctic Peninsula. *Tectonics*, **13**, 1345–1370.

MATTAUER, M. & MERCIER, J.L. 1980. Microtectonique et grande tectonique. *Bulletin Société Géologique de France*, **10**, 140–161.

NAKAMURA, K. & UYEDA, S. 1980. Stress in arc-back arc regions and plate subduction. *Journal of Geophysical Research*, **85**, 6419–6428.

PALLÀS, R. 1996. *Geologia de l'Illa de Livingston (Shetland del Sud, Antàrtida). Del Mesozoic al Present.* PhD thesis, Universitat de Barcelona. 265 pp. [Unpublished]

PALLÀS, R., MUÑOZ, J.A. & SÀBAT, F. 1992. Estratigrafía de la Formación Miers Bluff, Isla Livingston, Islas Shetland del Sur. *In* LÓPEZ-MARTÍNEZ, J., *ed. Geología de la Antártida Occidental.* Simposios T-3. Salamanca: III Congreso Geológico de España y VIII Congreso Latinoamericano de Geología, 105–115.

PALLÀS, R., VILAPLANA, J. M. & SÀBAT, F. 1995. Geomorphological and neotectonic features of Hurd Peninsula, Livingston Island, South Shetland Islands. *Antarctic Science*, **7**, 395–406.

PELAYO, A. & WIENS, D. 1989. Seismotectonics and relative plate motions in the Scotia Sea region. *Journal of Geophysical Research,* **94**, 7293–7320.

PRIETO, M.J., CANALS, M., ERCILLA, G., GRÀCIA, E. & DE BATIST, M. 1997. Sismoestratigrafía y edificación sedimentaria del margen SE y fondo de cuenca de la Cuenca Central de Bransfield (Antártida Occidental). *Boletín de la Real Sociedad Española de Historia Natural (Sección Geológica)*, **93**, 73–84.

RECHES, Z. 1987. Determination of the tectonic stress tensor from slip along faults that obey the Coulomb Yield condition. *Tectonics*, **6**, 849–861.

SÀBAT, F., SERRAT, D. & VILAPLANA, J.M. 1992. Cenozoic tectonic evolution in Livingston Island (South Shetlands, Antarctica): mesostructural and geomorphological approach. *Revista de la Sociedad Geológica de España*, **5**, 159–166.

SANTANACH, R., PALLÀS, F., SÀBAT, F. & MUÑOZ, J.A. 1992. La fracturación en la Isla Livingston, Islas Shetland del Sur. *In* LÓPEZ-MARTÍNEZ, J., *ed. Geología de la Antártida Occidental.* Simposios T-III. Salamanca: III Congreso Geológico de España y VIII Congreso Latinoamericano de Geología, 141–151.

SANTANACH, R., PALLÀS, F., SÀBAT, F. & MUÑOZ, J.A. 1996. From small scale to plate kinematics: paleostress determinations in a fragmented arc complex (SE Livingston Island, S. Shetland, Antarctica). *Journal of the Geological Society, London,* **153**, 1011–1020.

SASSI, W. & FAURE, J. 1996. Role of faults and layer interfaces on the spatial variation of stress regimes in basins: inferences from numerical modelling. *Tectonophysics*, **266**, 101–119.

SERVICIO GEOGRÁFICO DEL EJÉRCITO. 1991. *Isla Livingston. Base Antártica Española.* Mapa Topográfico Escala 1:5.000. Cartografía Antártica Española. Madrid: Servicio Geográfico del Ejército.

SERVICIO GEOGRÁFICO DEL EJÉRCITO. 1997. *Islas Livingston y Decepción, Islas Shetland del Sur.* Mapa Topográfico Escala 1:100.000. Cartografía Antártica Española. Madrid: Servicio Geográfico del Ejército.

SMELLIE, J.L., PANKHURST, R.J., THOMSON, M.R.A. & DAVIES, R.E.S. 1984. The geology of the South Shetland Islands: VI. Stratigraphy, geochemistry and evolution. *British Antarctic Survey Scientific Reports*, No. 85, 85 pp.

SMELLIE, J.L., LIESA, M., MUÑOZ, J.A., SÀBAT, F., PALLÀS, R. & WILLAN, R.C.R. 1995. Lithostratigraphy of volcanic and sedimentary sequences in central Livingston Island, South Shetland Islands. *Antarctic Science*, **7**, 99–113.

WALLACE, R.E. 1951. Geometry of shearing stress and relation to faulting. *Journal of Geology*, **59**, 118–130.

WILLAN, R.C.R. 1994. Structural setting and timing of hydrothermal veins and breccias on Hurd Peninsula, South Shetland Islands: a possible volcanic-related epithermal system in deformed turbidites. *Geological Magazine*, **131**, 465–483.

WILLAN, R.C.R., PANKHURST, R.J. & HERVÉ, F. 1994. A probable Early Triassic age for the Miers Bluff Formation, Livingston Island, South Shetland Islands. *Antarctic Science*, **6**, 401–408.